

See discussions, stats, and author profiles for this publication at: <https://www.researchgate.net/publication/263960385>

Fluorinated Porous Organic Polymers via Direct C–H Arylation Polycondensation

ARTICLE *in* ACS MACRO LETTERS · MAY 2013

Impact Factor: 5.76 · DOI: 10.1021/mz4001699

CITATIONS

20

READS

27

6 AUTHORS, INCLUDING:



Bao-Hang Han

National Center for Nanoscience and Techn...

100 PUBLICATIONS 3,868 CITATIONS

SEE PROFILE

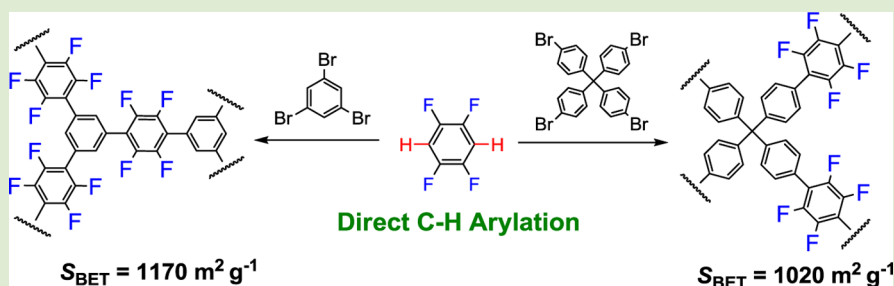
Fluorinated Porous Organic Polymers via Direct C–H Arylation Polycondensation

De-Peng Liu,^{†,‡} Qi Chen,^{*,‡} Yan-Chao Zhao,[‡] Li-Min Zhang,[‡] Ai-Di Qi,^{*,†} and Bao-Hang Han^{*,‡}

[†]College of Traditional Chinese Medicine, Tianjin University of Traditional Chinese Medicine, Tianjin 300193, China

[‡]National Center for Nanoscience and Technology, Beijing 100190, China

S Supporting Information



ABSTRACT: Considering the high reactivity of the C–H bonds in fluorobenzenes for direct arylation and special properties of fluorinated polymers, herein, synthesis of fluorinated porous organic polymers via direct C–H arylation polycondensation is explored. The obtained polymers (FPOP-1 and FPOP-2) are well characterized and show high porosities with Brunauer–Emmett–Teller specific surface area of above $1000 \text{ m}^2 \text{ g}^{-1}$. Different pore size distribution (PSD) profiles of porous polymers can be obtained by selecting different core constructing monomers. FPOP-2 exhibits a relatively narrower PSD with the dominant pore size at about 0.63 nm , which is more suitable for adsorption of small gas molecules (H_2 , CO_2 , and CH_4) than FPOP-1. As a porous fluorinated hydrophobic material, FPOP-2 possesses high adsorption ability for toluene (976 mg g^{-1} at saturated vapor pressure and room temperature) due to its high porosities and binding affinities between the guest molecules and the host network. The good sorption capacity of FPOP-2 for toluene makes it show potential applications in elimination of harmful small aromatic molecules in the environment.

Conjugated polymers with the unique optical and electrical properties have attracted much attention owing to their wide applications in organic thin-film solar cells,¹ organic electroluminescence devices,² and fluorescent sensors.³ Recently, porous conjugated polymers, as a special conjugated polymer with porosity, have been the hot field in porous material research.⁴ Porous conjugated polymers with intrinsic properties including large specific surface area, high chemical stability, and low skeleton density have exhibited potential applications in heterogeneous catalysis⁵ and gas storage and separation.⁶ Versatile porous organic polymers including porous conjugated polymers were obtained smoothly through a template-free chemical process by selection of proper building blocks and polymerization reactions, which show efficient preparation and high flexibility in the molecular design.⁷ Moreover, as for porous organic polymers, improvement of property and function can be accessible by functionalization approaches. For example, sulfonate or amine grafted porous polymer networks (PPNs) show higher CO_2 capture capacities than nongrafted polymers.⁸

Conventionally, many π -conjugated polymers including porous polymers were synthesized by polycondensation using transition-metal-catalyzed cross-coupling reactions such as the Suzuki coupling reaction and Sonogashira–Hagihara coupling

reaction.^{9,10} However, these methods usually require extra synthetic steps to prepare multifunctional monomers, and the effects of unavoidable residues derived from the monomer reactive groups (boric acid or alkyne) on the properties and functions of polymers are unclear.¹¹ In recent years, catalytic dehydrohalogenative cross-coupling reactions of nonpreactivated arenes or heteroarenes with aryl halides, known as direct arylation,¹² have been intensively investigated for the preparation of π -conjugated polymers with respect to improving the synthesis efficiency and reducing undesired waste. We focus on exploring the synthetic methodology and the properties of porous polymers.¹³ To our best knowledge, polycondensation via direct arylation has never been used in the preparation of a polymeric network with porosity. It is believed that direct arylation can expand the range of methods for the synthesis of porous organic polymers.

Because the acidic C–H bond affected by the fluorine substituents enables direct arylation more effective,¹⁴ Kanbara and Kuwabara have proven that the Pd-catalyzed polycondensation of tetrafluorobenzene with aryl halides via direct

Received: April 6, 2013

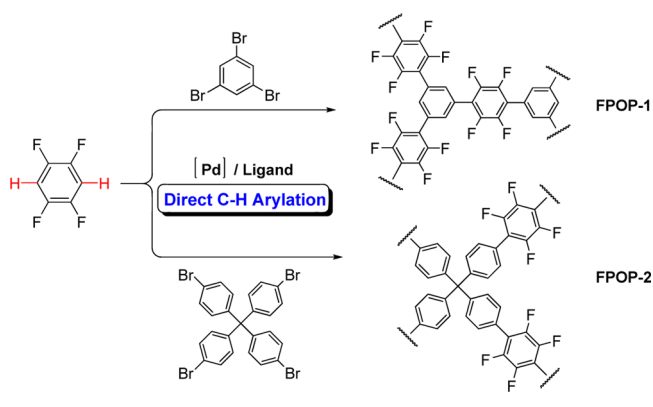
Accepted: May 29, 2013



arylation can afford a series of linear π -conjugated polymers consisting of fluorinated arylene units with excellent yields and high molecular weight.¹⁵ In addition, the byproducts (KBr, CO₂, and H₂O) of the polycondensation are easily removed from the polymer. Fluorinated porous poly(arylene-ethynylene)s have been prepared by Sonogashira–Hagihara coupling reaction and exhibit more hydrophobic nature than the nonfluorinated parent network.¹⁶ Considering the high reactivity of the C–H bonds in fluorobenzene for direct arylation and special properties of fluorinated polymers, herein, synthesis of fluorinated porous organic polymers via direct C–H arylation polycondensation is explored. The obtained polymers show high porosities with Brunauer–Emmett–Teller (BET) specific surface area of above 1000 m² g^{−1}. Their gas uptake and vapor adsorption capacities are also studied and discussed.

As shown in Scheme 1, the polycondensation of 1,2,4,5-tetrafluorobenzene with aryl bromides was carried out smoothly

Scheme 1. Preparation of Porous Organic Polymers FPOP-1 and FPOP-2



in the presence of Pd(OAc)₂ (5 mol %), a phosphine ligand P(*t*-Bu)₂Me-HBF₄ (10 mol %), and K₂CO₃ (2 equiv) in dimethylacetamide (DMAc) overnight, in which a combination of Pd(OAc)₂ and P(*t*-Bu)₂Me-HBF₄ is the most efficient catalytic system throughout the polymerization.^{15a} It has been explored as the optimal reaction condition for the polycondensation via direct arylation based on 1,2,4,5-tetrafluorobenzene.^{15b} By using the same method, the small molecule and linear polymer with similar repeating units have also been successfully prepared (see the Supporting Information), which means the structure of the repeating unit is stable under the reaction conditions. 1,3,5-Tribromobenzene and tetrakis(4-bromophenyl)methane have been selected as aryl bromides because the aromatic core structures derived from these two aryl bromides have been commonly used as building units to prepare conjugated microporous polymers (CMPs)^{10,17} or porous aromatic frameworks (PAFs),¹⁸ in which PAF-1, a microporous polyphenylene network first reported by Ben and co-workers, possesses an ultrahigh BET specific surface area up to 5640 m² g^{−1}.^{18a} The obtained polymers are chemically stable, even exposed to a dilute solution of acid or base, such as HCl or NaOH. Thermogravimetric analysis (Figure S1, Supporting Information) shows that the materials are stable up to 400 °C in all cases under nitrogen and has no evidence for distinct glass transition for these polymers below the thermal decomposition temperature owing to the nature of their cross-linking

structures, which is consistent with good physicochemical robustness for most of the porous organic polymers.⁴

To confirm their structures, the two polymers were characterized at the molecular level by ¹³C and ¹⁹F CP/MAS NMR. The ¹³C NMR spectra for the porous polymers with assignment of the resonances are shown in Figure 1. For

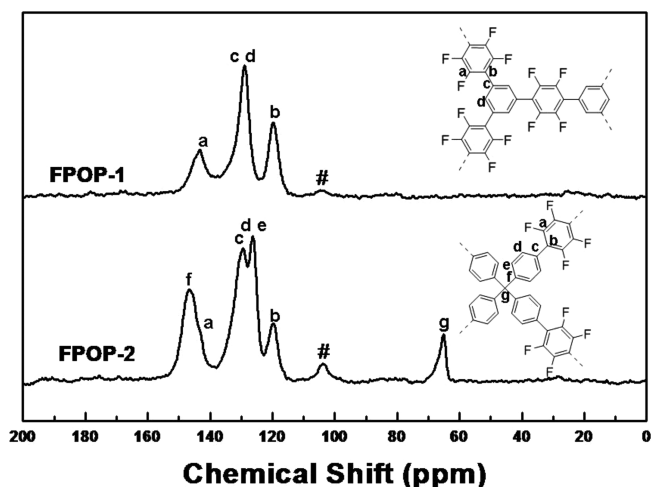


Figure 1. ¹³C CP/MAS NMR spectra of FPOP-1 and FPOP-2 (# denotes spinning sidebands).

FPOP-1, there are three broad peaks at about 143.4, 129.0, and 119.7 ppm, respectively. The peaks at 143.4 and 119.7 ppm correspond to the fluoro-substituted carbons and the phenyl-substituted carbons derived from monomer 1,2,4,5-tetrafluorobenzene, respectively. The signal peak of substituted and unsubstituted phenyl carbons from monomer 1,3,5-tribromobenzene is located at about 129.0 ppm. As for **FPOP-2**, the signal peak of quaternary carbons is observed at 65.1 ppm. The peak at 146.7 ppm corresponds to phenyl carbons linked to the quaternary carbon. Similar to **FPOP-1**, peaks at 143.2 and 119.7 ppm are ascribed to the fluoro-substituted carbons and the phenyl-substituted carbons derived from monomer 1,2,4,5-tetrafluorobenzene, respectively. The signal peaks of other phenyl carbons from monomer tetrakis(4-bromophenyl)methane are located at about 129.4 and 126.3 ppm. ¹⁹F NMR spectra of both polymers exhibit the signals of the repeating unit derived from monomer 1,2,4,5-tetrafluorobenzene at about −146.7 ppm (Figure S2, Supporting Information). We tested the two polymers with an SEM–EDXS (energy-dispersive X-ray spectrometer) analyzer and obtained the atom ratios of fluorine to carbon as about 1/3.0 for **FPOP-1** and 1/4.2 for **FPOP-2** (Figure 2), which are approximately consistent with the ratios (1/3.1 for **FPOP-1** and 1/4.7 for **FPOP-2**) by X-ray photoelectron spectroscopy (XPS) measurements (Figure S3, Supporting Information).

The porosity parameters of the polymers were studied by sorption analysis using nitrogen as the sorbate molecule. Nitrogen adsorption–desorption isotherms of **FPOP-1** and **FPOP-2** measured at 77 K are shown in Figure 3a, which exhibit a combination of type I and II nitrogen sorption isotherms according to the IUPAC classification.¹⁹ A rapid uptake at low relative pressure (*P*/*P*₀: 0–0.1) indicates a permanent microporous nature of two polymers. The increase in the nitrogen sorption at a high relative pressure above 0.9, for example, **FPOP-1**, may arise in part from interparticulate porosity associated with the meso- and macrostructures of the

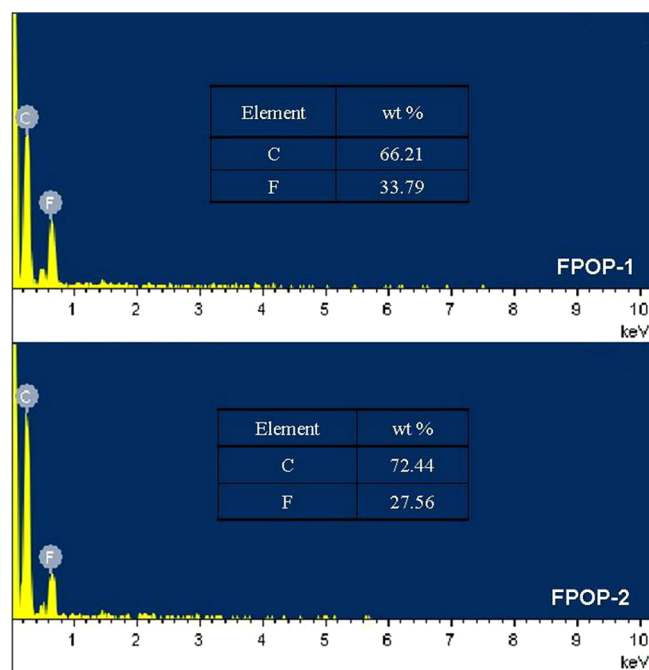


Figure 2. EDXS of FPOP-1 and FPOP-2 (the theoretical chemical formulas for FPOP-1 and FPOP-2 are $[C_{30}H_6F_{12}]_n$ and $[C_{37}H_{16}F_8]_n$, respectively).

samples and interparticular void.²⁰ Hysteresis can be observed apparently for FPOP-1 and FPOP-2 in the whole range of relative pressure based on the isotherms due to a linear increase of the adsorbed volume upon adsorption, which might be attributed to the swelling in a flexible polymer framework induced by adsorbate molecules dissolved in nominally nonporous parts of the polymer matrix after filling of open and accessible voids or the restricted access of adsorbate to the pores blocked by narrow openings.²¹

The specific surface area values calculated in the relative pressure (P/P_0) ranging from 0.01 to 0.1 according to the previous reports^{7a,13a} (Figure S4, Supporting Information) show that the BET specific surface area data of FPOP-1 and FPOP-2 range from 1020 to 1170 $m^2 g^{-1}$, which are comparable with some porous organic polymers obtained by other coupling polymerization methods such as Suzuki coupling reaction,^{13c} Sonogashira–Hagihara coupling reaction,^{6b} and Yamamoto reaction.^{17a} It is reasonable to comprehend that the high cross-linking density based on the rigid core structure monomers results in the polymers with stable, permanent pore structure and high specific surface area. PSD analysis based on the NLDFT approach has been used extensively to characterize a wide variety of porous materials although it does have some limitations.^{21b} The PSD profiles of polymers FPOP-1 and FPOP-2 were calculated from the adsorption branch of the isotherms with the NLDFT approach. As shown in Figure 3b, the pore sizes of polymer FPOP-1 dominantly range from 0.59 to 1.31 nm, associated with the mesoporous size distribution. Polymer FPOP-2 exhibits a narrow PSD with the dominant pore size at about 0.63 nm. This indicates that it is possible to control the PSD profile of porous polymers by selecting different core constructing monomers. Listed in Table 1 are the key structural properties of polymers, which are derived from the corresponding isotherm, such as the BET specific surface area, micropore surface area, pore volume, and dominant pore size. It should be

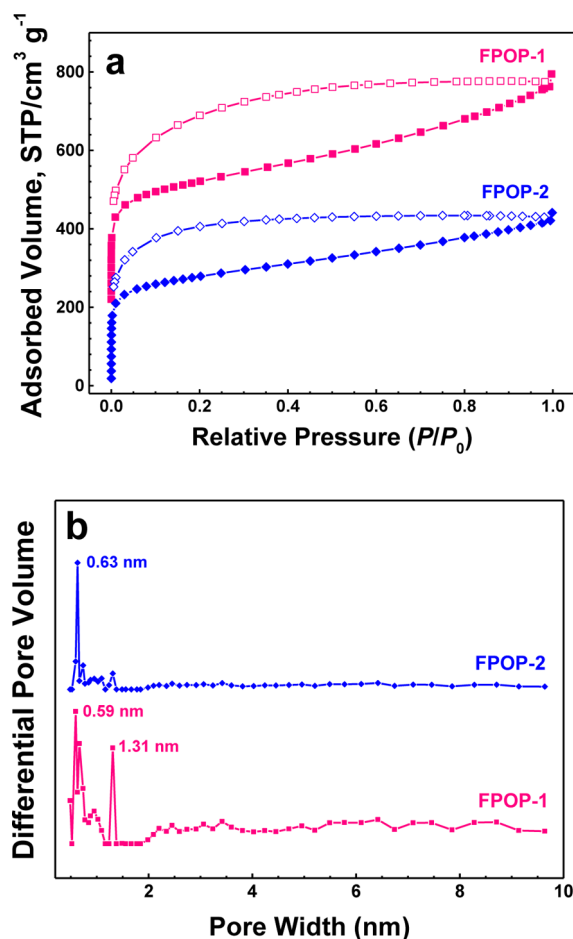


Figure 3. Nitrogen adsorption–desorption isotherms of FPOP-1 (pink) and FPOP-2 (blue) measured at 77 K (a) and related pore size distribution (PSD) profiles calculated by NLDFT (b). The adsorption and desorption branches are labeled with solid and open symbols, respectively. For clarity, the isotherms of FPOP-1 were shifted vertically by 200 $cm^3 g^{-1}$.

noted that the color of products with the similar repeating unit becomes darker and darker with the increase of repeating unit and porosity. According to the information related to product color, chemical structure, and porosity summarized in Table S1 (Supporting Information), it can be inferred that the black color of obtained porous polymers has a correlation with their cross-linking structure and porosity.

Microporous organic polymers with a narrow PSD may interact attractively with small gas molecules through improved molecular interaction. Therefore, the obtained microporous organic polymers inspired us to investigate their gas (H_2 , CO_2 , and CH_4) uptaking capacities. On the basis of the measured gas physisorption isotherms with pressure up to 1.13 bar (Figures S5a–c, Supporting Information), we can see that the obtained polymers show moderate uptaking capacities for hydrogen (1.05 wt % for FPOP-1 and 1.16 wt % for FPOP-2 at 1.0 bar and 77 K) and carbon dioxide (9.70 wt % for FPOP-1 and 10.2 wt % for FPOP-2 at 1.0 bar and 273 K), which are similar to some porous polymers.^{6b,22} The methane uptake of the polymers is also studied, and FPOP-2 exhibits a better uptake capacity (3.3 wt % at 1.0 bar and 273 K) than those of some porous materials with higher BET specific surface areas such as microporous polycarbazole CPOP-1,^{13a} MOF $Cu_2(ebtc)$,²³ porphyrin(Ni)-based porous polymer,²⁴ and adamantine-

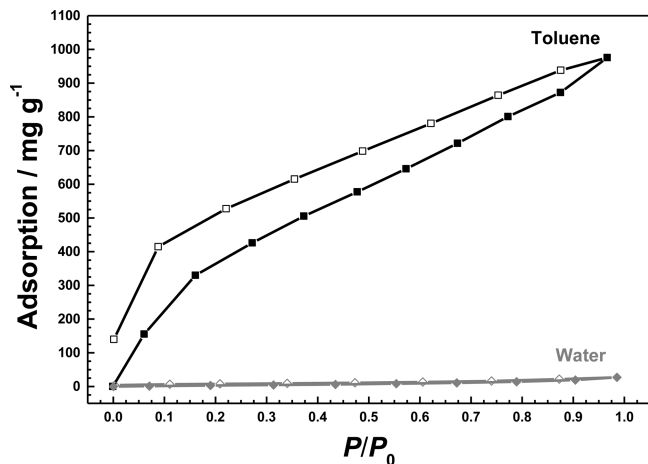
Table 1. Porosities and Gas Uptake Capacities of FPOP-1 and FPOP-2

polymers	S_{BET}^a ($\text{m}^2 \text{g}^{-1}$)	S_{micro}^b ($\text{m}^2 \text{g}^{-1}$)	V_{total}^c ($\text{cm}^3 \text{g}^{-1}$)	D_{pore}^d (nm)	CO_2 uptake ^e (wt %)	CH_4 uptake ^e (wt %)	H_2 uptake ^f (wt %)
FPOP-1	1170	577	0.870	0.59, 1.31	9.7	2.7	1.05
FPOP-2	1020	584	0.651	0.63	10.2	3.3	1.16

^aSpecific surface area calculated from the adsorption branch of the nitrogen adsorption–desorption isotherm using the BET method. ^bMicro pore surface area calculated from the adsorption branch of the nitrogen adsorption–desorption isotherm using the *t*-plot method. ^cTotal pore volume at $P/P_0 = 0.99$. ^dData calculated from nitrogen adsorption–desorption isotherms with the NLDFT method. ^eData were obtained at 1.0 bar and 273 K. ^fData were obtained at 1.0 bar and 77 K.

based porous polymer networks (PPN-2 and PPN-3) under the same conditions.²⁵ Moreover, the gas uptake capacities of FPOP-2 are correspondingly better than those of FPOP-1 with higher BET specific surface area under the same conditions (Table 1). Probably, it could be ascribed to the different PSD profiles. Unlike the pore sizes of FPOP-1 dominantly ranging from 0.59 to 1.31 nm with a combination of the mesoporous size distribution, FPOP-2 exhibits a relatively narrower PSD with the dominant pore size at about 0.63 nm, which is more suitable for adsorption of small gas molecules.^{13c}

Considering that the high porosities of the fluorinated polymers of FPOP-1 and FPOP-2 allow potential access by a variety of small molecules, we also explored the capability of FPOP-1 and FPOP-2 for adsorption of solvent vapors such as toluene and water. The sorption behaviors of toluene and water were measured at 298 K. As shown in Figure 4, FPOP-2

**Figure 4.** Toluene and water adsorption–desorption isotherms of FPOP-2 measured at 298 K.

features a typical type I isotherm for toluene, with a hysteresis that implies possible guest–host interaction might exist under relatively higher pressures²⁶ and is also likely to be a result of the presence of mesopores and capillary condensation. The adsorption of toluene rises gradually until the material reaches saturation, and the adsorption amount for toluene is 976 mg g^{-1} (10.6 mmol g^{-1}) at its saturated vapor pressure, which is higher than FPOP-1 (Figure S6, Supporting Information) and some reported porous materials such as PAF-11,^{18b} $[\text{Zn}_4\text{O}(\text{bdc})(\text{bpz})_2] \cdot 4\text{DMF} \cdot 6\text{H}_2\text{O}$,²⁵ and MOF based on a zinc(II) bipyridine-tetracarboxylate.²⁷ Though the sorption capacity of FPOP-2 for toluene is lower than that of PAF-1 (1357 mg g^{-1}),^{18a} FPOP-2 still exhibits good toluene sorption ability, considering the relatively lower specific surface area of FPOP-2 ($S_{\text{BET}} = 1020 \text{ m}^2 \text{g}^{-1}$) compared to PAF-1 ($S_{\text{BET}} = 5640 \text{ m}^2 \text{g}^{-1}$). The good sorption capacity of FPOP-2 for toluene could be ascribed to its high porosities and affinities between guest

molecules and the host network such as π – π , C–H $\cdots\pi$, and arene–perfluoroarene interactions.²⁸ This ability of FPOP-2 would be very promising to eliminate harmful small aromatic molecules in the environment. Meanwhile, the sorption capacity of FPOP-2 for water measured at saturation conditions and 298 K is only 27 mg g^{-1} (1.5 mmol g^{-1}), which is lower than hydrophobic porous polymer PAF-11^{18b} with similar nonfluorinated structure, and also proves the hydrophobic nature of the material. This result is consistent with Cooper's report, which is that the fluoro-substituted porous polymer shows more hydrophobic property than the parent network.¹⁶

In conclusion, based on the high reactivity of the C–H bonds in 1,2,4,5-tetrafluorobenzene for direct arylation, two fluorinated porous organic polymers (FPOP-1 and FPOP-2) were smoothly prepared via direct C–H arylation polycondensation and well characterized by solid-state ^{13}C and ^{19}F NMR, EDXS, and XPS. The obtained polymers show good thermal and chemical stabilities and high porosities with BET specific surface area of above $1000 \text{ m}^2 \text{g}^{-1}$. Different PSD profiles of the polymers can be obtained by selecting different core constructing monomers. Unlike the pore sizes of FPOP-1 dominantly ranging from 0.59 to 1.31 nm with a combination of the mesoporous size distribution, FPOP-2 exhibits a relatively narrower PSD with the dominant pore size at about 0.63 nm and shows better gas (H_2 , CO_2 , and CH_4) uptake capacities than FPOP-1 under the same conditions. Moreover, FPOP-2 also possesses high adsorption ability for toluene (976 mg g^{-1}) at saturated vapor pressure and room temperature due to its high porosities and binding affinities between guest molecules and the host network such as π – π , C–H $\cdots\pi$, and arene–perfluoroarene interactions. As a porous fluorinated hydrophobic material, FPOP-2 could find a potential use in elimination of harmful small aromatic molecules, which are of concern to the environment. Various fluorinated porous polymers have been prepared by this facile method, and the related porosities and special properties are under study.

■ ASSOCIATED CONTENT

Supporting Information

TGA, ^{19}F NMR spectra, XPS spectra, BET specific surface area plots, and gas (H_2 , CO_2 , and CH_4) adsorption isotherms of FPOP-1 and FPOP-2; toluene and water adsorption–desorption isotherms of FPOP-2 measured at 298 K. This material is available free of charge via the Internet at <http://pubs.acs.org>.

■ AUTHOR INFORMATION

Corresponding Author

*E-mail: hanbh@nanocr.cn; chenq@nanocr.cn; qiaidi@tjutc.edu.cn.

Notes

The authors declare no competing financial interest.

ACKNOWLEDGMENTS

The financial support of the National Science Foundation of China (Grants 21002017 and 21274033) and the Chinese Academy of Science (Grant KJCX2-YW-H21) is acknowledged.

REFERENCES

- (1) (a) Boudreault, P. L. T.; Najari, A.; Leclerc, M. *Chem. Mater.* **2011**, *23* (3), 456–469. (b) Chen, Y. J.; Yang, S. H.; Hsu, C. S. *Chem. Rev.* **2009**, *109* (11), 5868–5923.
- (2) (a) Grimsdale, A. C.; Chan, K. L.; Martin, R. E.; Jokisz, P. G.; Holmes, A. B. *Chem. Rev.* **2009**, *109* (3), 897–1091. (b) Huang, F.; Wu, H.; Cao, Y. *Chem. Soc. Rev.* **2010**, *39* (7), 2500–2521.
- (3) (a) Thomas, S. W.; Joly, G. D.; Swager, T. M. *Chem. Rev.* **2007**, *107* (4), 1339–1386. (b) Chen, Q.; Cui, Y.; Zhang, T.-L.; Cao, J.; Han, B.-H. *Biomacromolecules* **2010**, *11* (1), 13–19. (c) Chen, Q.; Cheng, Q.-Y.; Zhao, Y.-C.; Han, B.-H. *Macromol. Rapid Commun.* **2009**, *30* (19), 1651–1655.
- (4) (a) Cooper, A. I. *Adv. Mater.* **2009**, *21* (12), 1291–1295. (b) Dawson, R.; Cooper, A. I.; Adams, D. J. *Prog. Polym. Sci.* **2012**, *37* (4), 530–563.
- (5) (a) Zhang, Y.; Riduan, S. N. *Chem. Soc. Rev.* **2012**, *41* (6), 2083–2094. (b) Kaur, P.; Hupp, J. T.; Nguyen, S. B. T. *ACS Catal.* **2011**, *1* (7), 819–835.
- (6) (a) McKeown, N. B.; Budd, P. M. *Macromolecules* **2010**, *43* (12), 5163–5176. (b) Dawson, R.; Stockel, E.; Holst, J. R.; Adams, D. J.; Cooper, A. I. *Energy Environ. Sci.* **2011**, *4* (10), 4239–4245.
- (7) (a) Chen, Q.; Wang, J.-X.; Yang, F.; Zhou, D.; Bian, N.; Zhang, X.-J.; Yan, C.-G.; Han, B.-H. *J. Mater. Chem.* **2011**, *21* (35), 13554–13560. (b) Farha, O. K.; Spokoyny, A. M.; Hauser, B. G.; Bae, Y.-S.; Brown, S. E.; Snurr, R. Q.; Mirkin, C. A.; Hupp, J. T. *Chem. Mater.* **2009**, *21* (14), 3033–3035. (c) Mohammad, G. R.; El-Kaderi, H. M. *Chem. Mater.* **2011**, *23* (7), 1650–1653. (d) Schmidt, J.; Weber, J.; Epping, J. D.; Antonietti, M.; Thormas, A. *Adv. Mater.* **2009**, *21* (6), 702–705.
- (8) (a) Lu, W.; Yuan, D.; Sculley, J.; Zhao, D.; Krishna, R.; Zhou, H.-C. *J. Am. Chem. Soc.* **2011**, *133* (45), 18126–18129. (b) Lu, W.; Sculley, J. P.; Yuan, D.; Krishna, R.; Wei, Z.; Zhou, H.-C. *Angew. Chem., Int. Ed.* **2012**, *51* (30), 7480–7484.
- (9) Weber, J.; Thomas, A. *J. Am. Chem. Soc.* **2008**, *130* (20), 6334–6335.
- (10) Jiang, J. X.; Su, F.; Trewin, A.; Wood, C. D.; Campbell, N. L.; Niu, H.; Dickinson, C.; Ganin, A. Y.; Rosseinsky, M. J.; Khimyak, Y. Z.; Cooper, A. I. *Angew. Chem., Int. Ed.* **2007**, *46* (45), 8574–8578.
- (11) Lim, H.; Chang, J. Y. *Macromolecules* **2010**, *43* (17), 6943–6945.
- (12) (a) Ackermann, L.; Vicente, R.; Kapdi, A. R. *Angew. Chem., Int. Ed.* **2009**, *48* (52), 9792–9826. (b) Berrouard, P.; Najari, A.; Pron, A.; Gendron, D.; Morin, P. O.; Pouliot, J. R.; Veilleux, J.; Leclerc, M. *Angew. Chem., Int. Ed.* **2012**, *51* (9), 2068–2071.
- (13) (a) Chen, Q.; Luo, M.; Hammershøj, P.; Han, Y.; Laursen, B. W.; Yan, C.-G.; Han, B.-H. *J. Am. Chem. Soc.* **2012**, *134* (14), 6084–6087. (b) Zhao, Y.-C.; Cheng, Q.-Y.; Zhou, D.; Wang, T.; Han, B.-H. *J. Mater. Chem.* **2012**, *22* (23), 11509–11514. (c) Chen, Q.; Wang, J.-X.; Wang, Q.; Bian, N.; Li, Z.-H.; Han, B.-H. *Macromolecules* **2011**, *44* (20), 7987–7993. (d) Zhao, Y.-C.; Zhou, D.; Chen, Q.; Zhang, X.-J.; Bian, N.; Qi, A.-D.; Han, B.-H. *Macromolecules* **2011**, *44* (16), 6382–6388.
- (14) (a) Gorelsky, S. I.; Lapointe, D.; Fagnou, K. J. *J. Am. Chem. Soc.* **2008**, *130* (33), 10848–10849. (b) Do, H.-Q.; Daugulis, O. *J. Am. Chem. Soc.* **2008**, *130* (4), 1128–1129. (c) Fan, S.; Yang, J.; Zhang, X. *Org. Lett.* **2011**, *13* (16), 4374–4377.
- (15) (a) Lu, W.; Kuwabara, J.; Kanbara, T. *Macromolecules* **2011**, *44* (6), 1252–1255. (b) Lu, W.; Kuwabara, J.; Iijima, T.; Higashimura, H.; Hayashi, H.; Kanbara, T. *Macromolecules* **2012**, *45* (10), 4128–4133.
- (16) Dawson, R.; Laybourn, A.; Clowes, R.; Khimyak, Y. Z.; Adams, D. J.; Cooper, A. I. *Macromolecules* **2009**, *42* (22), 8809–8816.
- (17) (a) Schmidt, J.; Werner, M.; Thomas, A. *Macromolecules* **2009**, *42* (13), 4426–4429. (b) Holst, J. R.; Stockel, E.; Adams, D. J.; Cooper, A. I. *Macromolecules* **2010**, *43* (20), 8531–8538.
- (18) (a) Ben, T.; Rao, H.; Ma, S.; Cao, D.; Lan, J.; Jing, X.; Wang, W.; Xu, J.; Deng, F.; Simmons, J. M.; Qiu, S.; Zhu, G. *Angew. Chem., Int. Ed.* **2009**, *48* (50), 9457–9460. (b) Yuan, Y.; Sun, F.; Ren, H.; Jing, X.; Wang, W.; Ma, H.; Zhao, H.; Zhu, G. *J. Mater. Chem.* **2011**, *21* (35), 13498–13502.
- (19) Sing, K. S. W.; Everett, D. H.; Haul, R. A. W.; Moscou, L.; Pierotti, R. A.; Rouquérol, J.; Siemieniowska, T. *Pure Appl. Chem.* **1985**, *57* (4), 603–619.
- (20) Chen, Q.; Luo, M.; Wang, T.; Wang, J.-X.; Zhou, D.; Han, Y.; Yan, C.-G.; Han, B.-H. *Macromolecules* **2011**, *44* (14), 5573–5577.
- (21) (a) Rose, M.; Klein, N.; Böhlmann, W.; Böhringer, B.; Fichtner, S.; Kaskel, S. *Soft Matter* **2010**, *6* (16), 3918–3923. (b) Weber, J.; Schmidt, J.; Thomas, A.; Böhlmann, W. *Langmuir* **2010**, *26* (19), 15650–15656.
- (22) Germain, J.; Freché, J. M. J.; Svec, F. *Small* **2009**, *5* (10), 1098–1111.
- (23) Hu, Y.; Xiang, S.; Zhang, W.; Zhang, Z.; Wang, L.; Bai, J.; Chen, B. *Chem. Commun.* **2009**, *48*, 7551–7553.
- (24) Wang, Z.; Yuan, S.; Mason, A.; Reprogel, B.; Liu, D. J.; Yu, L. *Macromolecules* **2012**, *45* (18), 7413–7419.
- (25) Lu, W.; Yuan, D.; Zhao, D.; Schilling, C. I.; Plietzsch, O.; Müller, T.; Bräse, S.; Guenther, J.; Blümel, J.; Krishna, R.; Li, Z.; Zhou, H. C. *Chem. Mater.* **2010**, *22* (21), 5964–5972.
- (26) Hou, L.; Lin, Y. Y.; Chen, X. M. *Inorg. Chem.* **2008**, *47* (4), 1346–1351.
- (27) Lin, X.; Blake, A. J.; Wilson, C.; Sun, X. Z.; Champness, N. R.; George, M. W.; Hubberstey, P.; Mokaya, R.; Schroder, M. *J. Am. Chem. Soc.* **2006**, *128* (33), 10745–10753.
- (28) (a) Eddaoudi, M.; Li, H. L.; Yaghi, O. M. *J. Am. Chem. Soc.* **2000**, *122* (7), 1391–1397. (b) Kishikawa, K.; Oda, K.; Aikyo, S.; Kohmoto, S. *Angew. Chem., Int. Ed.* **2007**, *46* (5), 764–768.